Transport in MultiTerminal Normal-Superconductor Devices: Reciprocity Relations, Negative and Nonlocal Resistances, and Reentrance of the Proximity Effect

S. G. den Hartog, C. M. A. Kapteyn, B. J. van Wees, and T. M. Klapwijk
Department of Applied Physics and Materials Science Centre, University of Groningen, Nijenborgh 4, 9747 AG Groningen, The Netherlands

G. Borghs
Interuniversity Micro Electronics Centre, Kapeldreef 75, B-3030 Leuven, Belgium
(Received 11 June 1996)

We have investigated transport in a cross-shaped two-dimensional electron gas with superconducting electrodes coupled to two opposite arms. Multiterminal resistances, measured as a function of the superconducting phase difference and the magnetic flux, are analyzed in terms of an extended Landauer-Büttiker transport formalism. We show that extended reciprocity relations hold. Correlations between transport coefficients are obtained from, e.g., (negative) three-terminal and nonlocal resistances. Energy spectroscopy reveals a reentrant behavior of the transport coefficients around the Thouless energy. [S0031-9007(96)01821-2]

PACS numbers: 74.50.+r, 73.50.–h, 74.25.Fy

A renewed interest has grown in the proximity effect in normal-superconductor (NS) devices [1–4] and its relation to mesoscopic transport. A striking reentrant behavior was predicted, where the resistance of a diffusive normal conductor at low energies returns to the normal state resistance. These calculations are based on impurity-averaged Keldysh Green's function techniques. An alternative theoretical description is based on a scattering approach [5], which incorporates not only ensemble-averaged but sample-specific transport properties as well. The Landauer-Büttiker transport formalism [6] for normal conductors describes transport in terms of reflection coefficients R_{ii}^{ee} and transmission coefficients T_{ij}^{ee} from lead j to lead i. A multiterminal scattering approach has been proposed for transport in NS devices based on an extension of this formalism [7], including Andreev transmission and reflection coefficients $(T_{ij}^{he}, R_{ii}^{he})$. The current flowing in lead i is expressed as

$$I_i = \frac{2e}{h}\left[(N_i - R_{ii}^{ee} + R_{ii}^{he})\mu_i - \sum_{j\neq i}(T_{ij}^{ee} - T_{ij}^{he})\mu_j\right]. \quad (1)$$

Particle conservation implies $N_i = R_{ii}^{ee} + R_{ii}^{he} + \sum_{j\neq i} \times (T_{ji}^{ee} + T_{ji}^{he})$, where N_i denotes the number of quantum channels. The electrochemical potentials μ_i of the normal leads are defined relative to the electrochemical potential of the superconductors ($\mu_0 = 0$).

In this Letter, we will experimentally investigate multiterminal transport in a diffusive, cross-shaped two-dimensional electron gas (2DEG), where a superconducting loop is attached to two opposite arms (see Fig. 1). The presence of three independent leads within the phase-breaking length allows us to study the average magnitude and the superconducting phase and magnetic flux sensitivity of the transport coefficients and their correlations.

The 2DEG is present in an InAs/AlSb quantum well. Prior to processing, the top barrier has been removed by wet chemical etching. The 15 nm thick exposed InAs layer hosts the 2DEG with an electron density $n_s \simeq 1.5 \times 10^{16}$ m^{-2} and an electron mean free path $\ell_e \simeq 0.2$ μm. The cross-shaped pattern in the InAs layer was defined by insulating trenches using e-beam lithography and wet chemical etching. An insulating Si layer was deposited on top of regions 1 and 2 to prevent a short circuit with the subsequently deposited Nb superconducting loop. A high transparency of about 0.9 is obtained for the NS interfaces by *in situ* Ar cleaning of the exposed InAs regions before the Nb deposition.

We first derive an expression for the multiterminal resistances for the geometry shown in Fig. 1. We define the transport coefficients as the difference between the normal and Andreev transmission/reflection coefficients: $T_{ij} = T_{ij}^{ee} - T_{ij}^{he}$ and $R_{ii} = R_{ii}^{ee} - R_{ii}^{he}$. For the moment, we will describe regions A and B as reservoirs, assuming

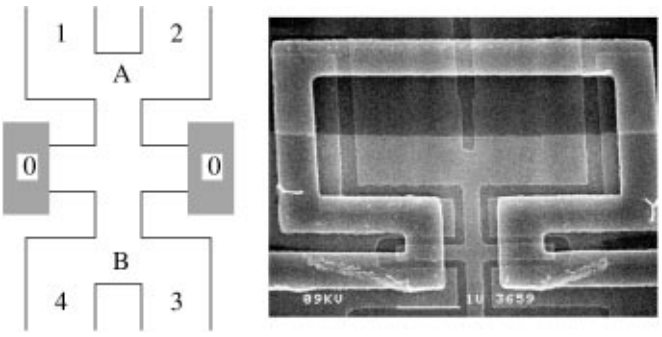

FIG. 1. Sample layout. The left-hand panel shows a schematic picture of the cross-shaped 2DEG with the superconducting terminals. The contacts 1, 2, 3, and 4, are connected to the cross-shaped 2DEG and the superconducting contacts 0 are connected to the Nb loop. The length of the InAs channel connecting the Nb terminals is $L \simeq 0.9$ μm and its width is $W \simeq 0.25$ μm. The right-hand panel shows a scanning electron micrograph.

 0031-9007/96/77(24)/4954(4)$10.00

uniform electrochemical potentials $\mu_A = \mu_1 = \mu_2$ and $\mu_B = \mu_3 = \mu_4$, respectively. We then obtain [8]

$$\mathcal{R}_{10,20} = \frac{h}{2e^2} \frac{N - R_{BB}}{(N - R_{AA})(N - R_{BB}) - T_{AB}T_{BA}}, \quad (2)$$

$$\mathcal{R}_{30,40} = \frac{h}{2e^2} \frac{N - R_{AA}}{(N - R_{AA})(N - R_{BB}) - T_{AB}T_{BA}}, \quad (3)$$

$$\mathcal{R}_{10,30} = \frac{h}{2e^2} \frac{T_{BA}}{(N - R_{AA})(N - R_{BB}) - T_{AB}T_{BA}}, \quad (4)$$

$$\mathcal{R}_{30,10} = \frac{h}{2e^2} \frac{T_{AB}}{(N - R_{AA})(N - R_{BB}) - T_{AB}T_{BA}}. \quad (5)$$

The number of quantum channels is given by $N = k_F W/\pi$, where W is the width of the arms of the cross. We will refer to Eqs. (2) and (3) as "two-terminal" resistances, since they effectively measure the resistance between region A (or B) and the Nb electrodes. Equations (4) and (5) represent "three-terminal" resistances, since they involve both regions A and B and the Nb electrodes.

Time-reversal symmetry implies for the transport coefficients that $T_{ij}(\Phi, \Delta\varphi) = T_{ji}(-\Phi, -\Delta\varphi)$ and $R_{ii}(\Phi, \Delta\varphi) = R_{ii}(-\Phi, -\Delta\varphi)$ [7], where Φ is the magnetic flux through the conductor and $\Delta\varphi$ is the superconducting phase difference across the two Nb terminals. The reciprocity relations can be derived from the extended Landauer-Büttiker formalism [Eq. (1)]: $\mathcal{R}_{ij,kl}(\Phi, \Delta\varphi) = \mathcal{R}_{kl,ij}(-\Phi, -\Delta\varphi)$. Interchanging current and voltage leads accompanied by a sign reversal in *both* Φ *and* $\Delta\varphi$ is predicted to yield the same resistance.

The magnetoresistances for the two- and three-terminal configurations are shown in Fig. 2. An applied magnetic field B changes the superconducting phase difference $\Delta\varphi$ linearly: $\Delta\varphi = 2\pi\Phi_{\text{loop}}/\Phi_0$, where Φ_{loop} is the magnetic flux through the superconducting loop (area $\simeq 13.6\ \mu$m) and Φ_0 is the flux quantum $h/2e$. Simultaneously, a magnetic flux Φ penetrates the cross-shaped conductor itself, and changes the quantum interference.

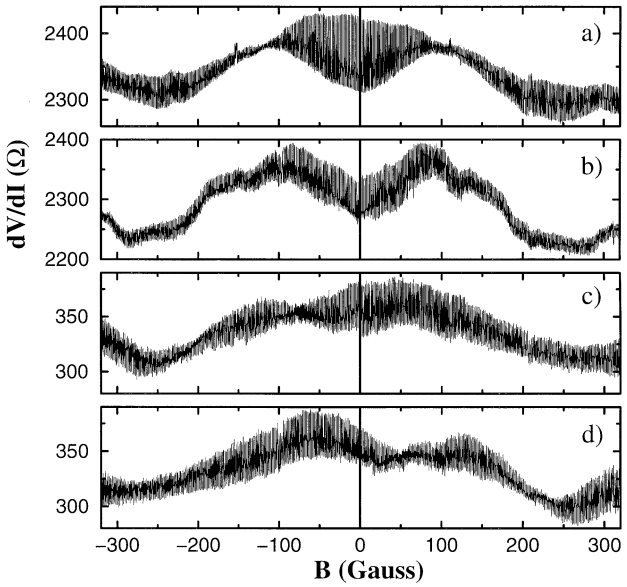

FIG. 2. The two-terminal magnetoresistances $\mathcal{R}_{10,20}$ (a) and $\mathcal{R}_{30,40}$ (b). The three-terminal magnetoresistances $\mathcal{R}_{10,30}$ (c) and $\mathcal{R}_{30,10}$ (d) measured simultaneously with the two-terminal magnetoresistances at $T \simeq 100$ mK.

We have investigated six nominally identical devices and studied two of them extensively at 100 mK with a standard four-probe ac lock-in technique and filtered leads. The magnetoresistance shows oscillations (period $\simeq 1.65$ G) due to superconducting phase modulated conductance fluctuations, superimposed on a fluctuating background resistance [4,9]. At low magnetic fields (<100 G) a nonsample specific (ensemble-averaged) contribution to the resistance oscillations is present. Evidently, the two-terminal resistances $\mathcal{R}_{10,20}$ and $\mathcal{R}_{30,40}$, as shown in Figs. 2(a) and 2(b), are symmetric in Φ and $\Delta\varphi$. The three-terminal magnetoresistance $\mathcal{R}_{10,30}$ [Fig. 2(c)] is asymmetric. This asymmetry is indeed reversed when the current and voltage probes are interchanged [$\mathcal{R}_{30,10}$ in Fig. 2(d)]. Closer inspection of the oscillations also shows that their phase changes sign under the reversal of current and voltage probes (not displayed).

Analyzing data acquired over a large range in magnetic field ($|B| \leq 0.5$ T) with Eqs. (2)–(5), we can estimate the values for the transport coefficients and their fluctuations. We obtain (with $N \simeq 35$) for the average transport coefficients $\langle R_{AA}\rangle \simeq 26$ and $\langle T_{BA}\rangle \simeq 1.6$, for the rms amplitude of the fluctuations $\Delta R_{AA} \simeq 0.26$ and $\Delta T_{BA} \simeq 0.07$ with a correlation magnetic field [4] $B_c \simeq 200$ and 130 G, respectively, and for the rms amplitude of the oscillations $\delta R_{AA} \simeq 0.012$ and $\delta T_{BA} \simeq 0.014$, both with $B_c \simeq 60$ G. Both ΔR_{AA} and ΔT_{BA} are somewhat smaller than expected from the theory of universal conductance fluctuations [10]. The reduction in ΔT_{BA} compared to ΔR_{AA} [11] implies either that the fluctuations in *both* T_{BA}^{ee} *and* T_{BA}^{he} are small or, more likely, that the fluctuations in T_{BA}^{ee} and T_{BA}^{he} are (partially) correlated. Also, $\delta R_{AA} \ll \Delta R_{AA}$ and $\delta T_{BA} \ll \Delta T_{BA}$, indicating that the conductance fluctuations are only partially modulated by the superconducting phase.

A striking manifestation of the coexistence of Andreev and normal transmission is displayed in Fig. 3(a). It follows from Eq. (4) that $\mathcal{R}_{10,30}$ is proportional to $T_{BA} = T_{BA}^{ee} - T_{BA}^{he}$. This implies that when an incoming electron has a higher probability to be transmitted as a hole than as an electron ($T_{BA}^{he} > T_{BA}^{ee}$), $\mathcal{R}_{10,30}$ can become *negative* [12]. Note that negative three-terminal resistances are impossible in normal transport, since, in that case, a voltage probe always measures a voltage in between that of the current source and drain contacts. As a result of a relatively high overall resistance of this device ($\mathcal{R}_{10,20} \simeq 10\ \text{k}\Omega$), the sample-specific fluctuations are increased and become of the order of the average three-terminal resistance $\mathcal{R}_{10,30}$ ($\langle T_{BA}\rangle \simeq 0.024$, $\Delta T_{BA} \simeq 0.007$, and $\delta T_{BA} \simeq 0.003$). The three-terminal magnetoresistance becomes negative around 290 G, indicating that the Andreev transmission dominates over normal transmission.

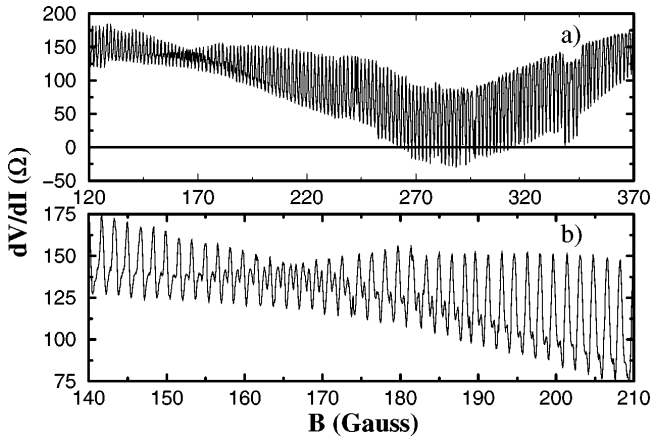

FIG. 3. (a) The three-terminal magnetoresistance $\mathcal{R}_{10,30}$ at $T \simeq 100$ mK of a device with an increased overall resistance ($\mathcal{R}_{10,20} \simeq 10$ kΩ). Around 290 G the resistance becomes negative. Note the cross over between two different Andreev-mediated oscillation patterns in (b).

Near 170 G a crossover takes place between two different oscillation patterns [Fig. 3(b)]. Several of these crossovers, which are sample specific, are observed with a typical separation of ~160 G. At present, we do not understand the underlying physical mechanism. However, this crossover cannot be described by a superposition of independent sinusoidal oscillation patterns in T_{BA}^{ee} and T_{BA}^{he}. An estimation of their average magnitude ($\langle T_{BA}^{ee} \rangle \simeq 0.32$ and $\langle T_{BA}^{he} \rangle \simeq 0.29$ [13]) for this device shows that they are equally important. In principle, either T_{BA}^{ee} or T_{BA}^{he} could still dominate the amplitude of the oscillations. More likely, their amplitudes have the same order of magnitude, which implies that the crossovers should be present in both T_{BA}^{ee} and T_{BA}^{he} [14].

A further interesting phenomenon in normal mesoscopic transport was the occurrence of nonlocal transport. The resistance of a phase-coherent metal strip connected at one end to a loop revealed Aharonov-Bohm oscillations, although no net current was flowing through the loop itself [15]. We searched for the superconducting-phase modulation of the nonlocal resistance by measuring the resistance $\mathcal{R}_{10,34}$. If region B is phase coherent, we have to treat contact 3 and 4 explicitly. A current flow from region A to the Nb contacts then yields the following nonlocal (four-terminal) resistance:

$$\mathcal{R}_{10,34} \simeq \frac{h}{2e^2} \frac{2(T_{3A} - T_{4A})}{T_{43} + T_{34}}. \qquad (6)$$

A nonlocal resistance is thus expected if $T_{3A} \neq T_{4A}$. Figure 4 shows that, indeed, a nonlocal resistance is observed. From the rms amplitude of the fluctuations in $\mathcal{R}_{10,34}$, we obtain $\Delta(T_{3A} - T_{4A}) \simeq 0.003$ with an estimated $\langle T_{34} \rangle \simeq \langle T_{43} \rangle \approx 20$, which is much smaller than the fluctuations in the total transmission from A to B ($\Delta T_{BA} \simeq 0.07$). Therefore, either the fluctuations in T_{3A} and T_{4A} are (strongly) correlated, or the phase-coherence length does not fully extend to the contacts 3 and 4.

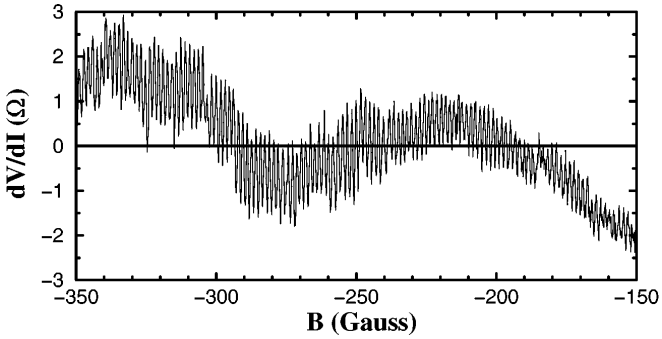

FIG. 4. The nonlocal four-terminal magnetoresistance $\mathcal{R}_{10,34}$ at $T \simeq 100$ mK (where $\mathcal{R}_{10,20} \simeq 3.5$ kΩ).

The above analysis, based on transport at the Fermi energy, has shown that the modulation in the two-terminal resistances is dominated by R_{AA} or R_{BB}, respectively [Eq. (2) or (3)]. In Fig. 5(a) the energy dependence of the magnitude of the oscillations in $\mathcal{R}_{10,20}$ is plotted, which reflects mainly the energy dependence of δR_{AA}. The oscillations in R_{AA} exhibited a *minimum* at $\Delta\varphi = 0$ as expected for coherent Andreev backscattering [2,5]. Dephasing of coherent quantum interference is expected to occur above the Thouless energy, estimated to be $E_T = \hbar v_F \ell_e / 2L^2 \simeq 0.1$ meV, which explains qualitatively the decrease in $\delta\mathcal{R}_{10,20}$ [Fig. 5(a)] for applied biases V_{DC} exceeding E_T. For $eV_{\mathrm{DC}} < E_T$, $\delta\mathcal{R}_{10,20}$ is reduced (a similar reduction was observed in Ref. [4]) and,

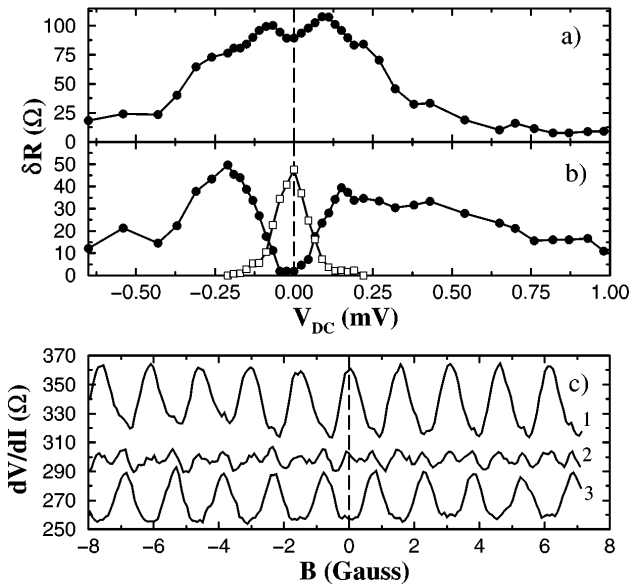

FIG. 5. The energy dependence of the (top-top) magnitude of the oscillations in $\mathcal{R}_{10,20}$ (a) and $\mathcal{R}_{10,30}$ (b) around zero magnetic field at $T \simeq 100$ mK (where $\mathcal{R}_{10,20} \simeq 2.2$ kΩ). In (b) the squares correspond to the component, which has a maximum in $\mathcal{R}_{10,30}$ at $\Delta\varphi \simeq 0.05\pi$. The circles correspond to the component, which has a minimum in $\mathcal{R}_{10,30}$ at $\Delta\varphi \simeq -0.01\pi$. (c) This shows $\mathcal{R}_{10,30}$ for three applied dc biases V_{DC}: 1—0 mV, 2—0.07 mV (offset −10Ω), and 3—0.13 mV (offset −20Ω).

simultaneously, the nonsinusoidal shape of the oscillations increases (not displayed). Calculations [2] show that for energies smaller than about E_T the amplitude of the oscillations is reduced, and a nonsinusoidal phase dependence develops [16].

The energy dependence of $\delta\mathcal{R}_{10,30}$ is governed by the energy dependence of δT_{BA} [Eq. (4)]. Near zero applied bias, the oscillations in $\mathcal{R}_{10,30}$ showed a *maximum* at $\Delta\varphi \simeq 0.05\pi$. For energies $eV_{\mathrm{DC}} \geq E_T$ these oscillations disappear [Fig. 5(b)]. Simultaneously, however, a contribution to the oscillations in $\mathcal{R}_{10,30}$ appears, which displays a *minimum* when $\Delta\varphi \simeq -0.01\pi$ and reaches its full magnitude at $eV_{\mathrm{DC}} \simeq E_T$. A similar behavior was observed in a second device with slightly different values for $\Delta\varphi$ (-0.03π and 0.02π, respectively). We conclude that these oscillations are dominated by an ensemble-averaged contribution with a small sample-specific contribution, which can account for the small deviations from $\Delta\varphi = 0$. We have plotted in Fig. 5(b) the magnitude of both types of oscillations. In Fig. 5(c) this crossover is illustrated by magnetic field traces for applied biases of 0, 0.07, and 0.13 mV. Note that the middle trace ($V_{\mathrm{DC}} \simeq$ 0.07 mV) exhibits both types of oscillations. Presently, no calculations for the energy dependence of transmission coefficients are available. We note, however, that these results are not in agreement with existing theories [2] for diffusive conductors. These predict that the position-dependent diffusion constant at zero energy is equal to its normal state value. This implies that the oscillation amplitude should vanish completely for $eV_{\mathrm{DC}} \ll E_T$, irrespective of the geometry. We conjecture that this discrepancy is related to the fact that the ratio of L/ℓ_e is not large in our devices.

We thank P. W. Brouwer, J. P. Heida, and A. F. Morpurgo for valuable discussions. This work is financially supported by FOM/NWO and KNAW (B. J. v. W.).

Note added.—A circuit theory analysis [2], in which we accounted for the finite ratio of L/ℓ_e by including ballistic point contacts in a series with the arms of the cross structure, can explain the observed magnitude and opposite phase of the oscillations in $\mathcal{R}_{10,30}$ near $B = 0$ at zero energy.

[1] S. N. Artemenko, A. F. Volkov, and A. V. Zaitsev, Solid State Commun. **30**, 771 (1979); A. F. Volkov, A. V. Zaitsev, and T. M. Klapwijk, Physica (Amsterdam) **210C**, 21 (1993); S. Yip, Phys. Rev. B **52**, 15 504 (1995).

[2] Y. V. Nazarov, Phys. Rev. Lett. **73**, 1420 (1994); Y. V. Nazarov and T. H. Stoof, Phys. Rev. Lett. **76**, 823 (1996); A. F. Volkov, N. Allsopp, and C. J. Lambert, J. Phys. Condens. Matter **8**, 45 (1996); A. A. Golubov, F. Wilhelm, and A. D. Zaikin (to be published).

[3] V. T. Petrashov *et al.*, Phys. Rev Lett. **74**, 5268 (1995); H. Courtois *et al.*, Phys. Rev Lett. **76**, 130 (1996); S. Guéron *et al.*, Phys. Rev Lett. **77**, 3025 (1996); P. Charlat *et al.* (to be published).

[4] S. G. den Hartog *et al.*, Phys. Rev. Lett. **76**, 4592 (1996).

[5] Y. Takane and H. Ebisawa, J. Phys. Soc. Jpn. **61**, 2858 (1992); C. W. J. Beenakker, Phys. Rev B **46**, 12 841 (1992); I. K. Marmorkos, C. W. J. Beenakker, and R. A. Jalabert, Phys. Rev. B **48**, 2811 (1993); C. W. J. Beenakker, J. A. Melsen, and P. W. Brouwer, Phys. Rev. B **51**, 13 883 (1995); N. R. Claughton, V. C. Hui, and C. J. Lambert, Phys. Rev. B **51**, 11 635 (1995); N. Argaman and A. Zee, Phys. Rev. B **54**, 7406 (1996).

[6] R. Landauer, Philos. Mag. **21**, 863 (1970); M. Büttiker, Phys. Rev. Lett. **57**, 1761 (1986); A. D. Benoit *et al.*, Phys. Rev. Lett. **57**, 1765 (1986); M. Büttiker, Phys. Rev. B **38**, 9375 (1988); B. J. van Wees *et al.*, Phys. Rev. B **43**, 12 431 (1991).

[7] C. J. Lambert, V. C. Hui, and S. J. Robinson, J. Phys. Condens. Matter **5**, 4187 (1993); B. J. van Wees, K. M. H. Lensen, and C. J. P. M. Harmans, Phys. Rev. B **44**, 470 (1991); M. P. Anantram and S. Datta, Phys. Rev. B **53**, 16 390 (1996).

[8] The indices display the actual current and voltage leads.

[9] B. L. Al'tshuler and B. Z. Spivak, Sov. Phys. JETP **65**, 343 (1987); P. W. Brouwer and C. W. J. Beenakker (to be published).

[10] B. L. Al'tshuler, JETP Lett. **41**, 648 (1985); P. A. Lee and A. D. Stone, Phys. Rev. Lett. **55**, 1622 (1985).

[11] A small reduction in ΔT_{BA} compared with ΔR_{AA} can be expected. Assuming mutually uncorrelated transport coefficients, $\Delta R_{ii}^{ee} \simeq 1$ and $\Delta R_{ii}^{he} \simeq \Delta T_{ij}^{ee} \simeq \Delta T_{ij}^{he} \simeq 1/\sqrt{3}$ resulting in $\Delta R_{ii} \simeq \sqrt{4/3}$ and $\Delta T_{ij} \simeq \sqrt{2/3}$.

[12] N. K. Allsopp *et al.*, J. Phys. Condens. Matter **6**, 10 475 (1994).

[13] Here we use that $\langle T_{BA}^{ee}\rangle + \langle T_{BA}^{he}\rangle \simeq 0.5(N - \langle R_{AA}\rangle)$.

[14] Recently, P. W. Brouwer *et al.* (unpublished) numerically obtained similar crossovers in a chaotic Josephson junction for both T_{BA}^{ee} and T_{BA}^{he}.

[15] C. P. Umbach *et al.*, Appl. Phys. Lett. **50**, 1289 (1987).

[16] In principle, a circulating supercurrent I_c could also be responsible for this nonsinusoidal phase dependence [B. J. van Wees *et al.*, Phys. Rev. Lett. **76**, 1402 (1996)]. However, this would require $I_c > 10\ \mu$A, which is much higher than observed by us in similar sized devices $I_c < 1\ \mu$A.